

# Modified Becke-Johnson calculations applied to the electronic and optical properties of Mg and Mn doped PbS

A. GASSOUMI<sup>a,b\*</sup>, A. AL-SHAHRANI<sup>a</sup>, S. ALFAIFY<sup>a</sup>, H. ALGARNI<sup>a</sup>, R. VIDU<sup>c</sup>

<sup>a</sup>King Khalid University, Faculty of Science, Department of Physics, P.O. Box 9004, Abha 61413, Saudi Arabia

<sup>b</sup>Université de Tunis El Manar, Faculté des Sciences de Tunis, Laboratoire de Physique de la Matière Condensée, 2092 Tunis, Tunisia

<sup>c</sup>University of California, Department of Chemical Engineering and Materials Science, Davis, CA 95616, United States

In this paper, electronic and optical properties of magnesium (Mg) and manganese (Mn) doped lead sulfide (PbS) compounds have been investigated based on the full-potential linear augmented plane wave (FP-LAPW) method by using the modified Becke-Johnson (mBJ) method. The detailed optical studied revealed that the band gap of pure PbS was found to be  $-0.9$  eV and Mg doped PbS exhibited direct band gap energy of  $\sim 2$  eV. Further, Mn doped PbS possess a metallic behavior. The PbS compound possess a cubic rock-salt structure with the space group Fm-3m and lattice parameter  $a = 5.931 \text{ \AA}$ , which were used in our calculations. The optical parameters, such as dielectric constant, refractive index and reflectivity were analyzed. The results demonstrated that Mg and Mn doped PbS compounds have the potential to be used for optoelectronic applications.

(Received February 16, 2018; accepted October 10, 2018)

**Keywords:** Mg and Mn doped PbS; Electronic properties; Optical properties

## 1. Introduction

Lead sulfide PbS, as one of the most important IV–VI group semiconductors with a large Bohr radius (18 nm), has attracted considerable interest in the recent years due to its promising applications in IR detection, decorative coatings, photo-thermal conversion for solar energy, and solar control coatings [1,2]. Lead sulphide has shown strong electron-holes quantum confinement, this causes multiple exciton generation leading to an enhancement in the photo-conversion efficiency of solar cells. One of the key requirements for many of these desired applications is the property induced by doping of PbS with various transition metal elements [3-6]. Hence, on that view, the doping of PbS with transition metal elements such as Mg, Zn and Cu have been studied by our group and published elsewhere [7–9]. A simple way to modify the properties of PbS is by systematic doping, with magnesium and manganese. The theoretical methods such as density functional theory (DFT) provide an extremely valuable tool for predicting different properties of a large number of semiconductors. In this work, we aim to establish theoretical means for a comprehensive understanding of the fundamental physical properties of Mn and Mg doped PbS for their potential use in advanced optoelectronic materials.

Recently  $\text{Mg}^{2+}$  ion has been used as doping in our experimental work [7] because of its outstanding properties such as small ionic radius (0.066 nm), p-type conductivity and large activation energy [10,11].

On the other hand,  $\text{Mn}^{2+}$  ion-doped has received increasing attention due to their potential applications in quantum computing, spintronic, and magneto-optics [5,12].

Moreover, the DFT calculation can serve as a predictive tool to development of new materials. However, the main limitation of theoretical study is the ability to produce the band gap of semiconductors in good agreement with that of experimental measurement due to exchange–correlation terms.

Furthermore, first principles calculations based on the density functional theory (DFT) using the common LDA and GGA usually underestimates the band gap energy as mentioned in Ref. [13,14]. Some moderate methods have recently been developed to correct band gap error such as modified Becke–Johnson (mBJ). This yield a band gap value less underestimated to experimental result. In our work, we use the modified Becke–Johnson (mBJ) approach, because it is more effective for the band gap calculations for semiconductors [15]. In our calculations, we used PbS with a cubic rock-salt structure, space group Fm-3m and lattice parameter  $a = 5.931 \text{ \AA}$  [16]. We believe that this study will help understand the fundamental properties of the designated materials and may improve their potential applications for many other engineered materials and technologies.

## 2. Computational methods

In this study, all the calculations for Mg and Mn doped PbS have been performed using the density functional theory (DFT) [17], based on the full-potential linearized augmented plane wave (FP-LAPW) method [18]. We have performed the calculations using a WIEN2K package [19]. We have applied the modified Becke-Johnson (mBJ) functional for the electronic structure and optical properties calculations. The convergence parameter  $R_{MT} \cdot K_{max}$  was equal to 8 and the  $I_{max}$  was equal to 10. The Fourier expansion of charge density was up to  $G_{max}=12$  (a.u.)<sup>-1</sup>. Less than 0.10 mRy of the self-consistency calculation of total energy has been used in this work. We constructed a  $2 \times 2 \times 2$  supercell, containing 32 atoms: 16 of Pb and 16 of S atoms, respectively. The doping of PbS was done by substituting one Pb atom by Mg or Mn atom in the supercell, which is produced a 3.125% doping concentration.

## 3. Results and discussion

### 3.1. Electronic properties

In order to understand the electronic properties of pure and Mg or Mn doped PbS in the  $2 \times 2 \times 2$  supercell (that corresponds to level doping of 3.125%), the band structures and the densities of states (DOS) are investigated with mBJ potential. In Fig. 1, it presented the

three band structures for pure PbS and for Mg and Mn doped PbS in the high symmetry direction in the BZ, the Fermi level ( $E_F$ ) is chosen to locate at ( $E = 0.0$  eV) and coincide with the top of the valence band (VB). It is observed from Fig. 1(a), that the calculated direct band gap of pure PbS is 0.9 eV. Fig. 1(b) shows that our results of the band structure calculations demonstrate that the Mn doped PbS material presents a metallic behavior which is in good agreement with other previous calculations [20], while Mg doped PbS reveals a semiconducting nature with a band gap of about 2eV ( see Fig. 1(c)), which is close to the experimental data [21]. When the Mg is doped in PbS, the Fermi level shifts down into the valence band, which produce a degenerate p-type semiconductor. To remind, in this effect, the band gap is measured between the conduction band minimum (CBM) and the Fermi level in the valence band. The energy distributions of the electronic states can be actually investigated by calculating the density of states (DOS). Since the optical spectra are calculated from the interband transitions, the total density of states (TDOS) along with the partial (PDOS) for Mn and Mg doped PbS are shown in Fig. 2 and Fig. 3, respectively. The valence band below the Fermi level ( $E_F$ ) consists of different regions, where the lower part situated between -5.0 and -1.0 eV is mainly due to the S-p states. Above the Fermi level ( $E_F$ ), the conduction band with positive energies is composed mainly of Pb-p states. When we substitute one Pb atom with one Mn or Mg atom, we find that, the Mn-p and Mg-s orbitals contributes to the occupied states around Fermi level.

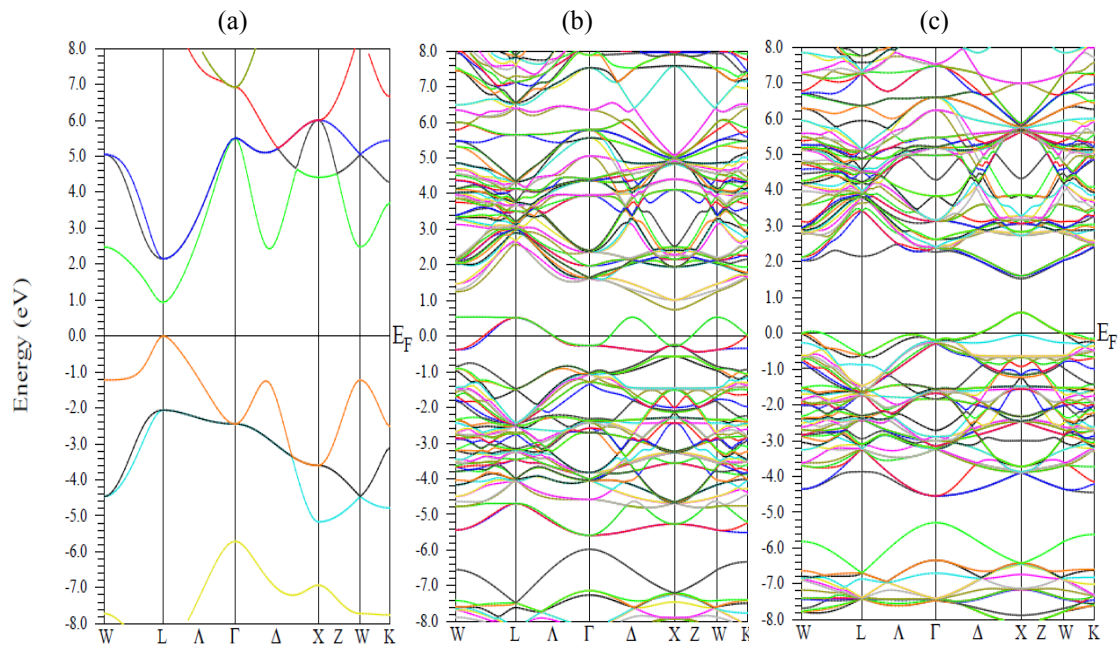


Fig. 1. Band structure of (a) pure PbS (b) Mn doped PbS in  $2 \times 2 \times 2$  supercell (c) Mg doped PbS in  $2 \times 2 \times 2$  supercell

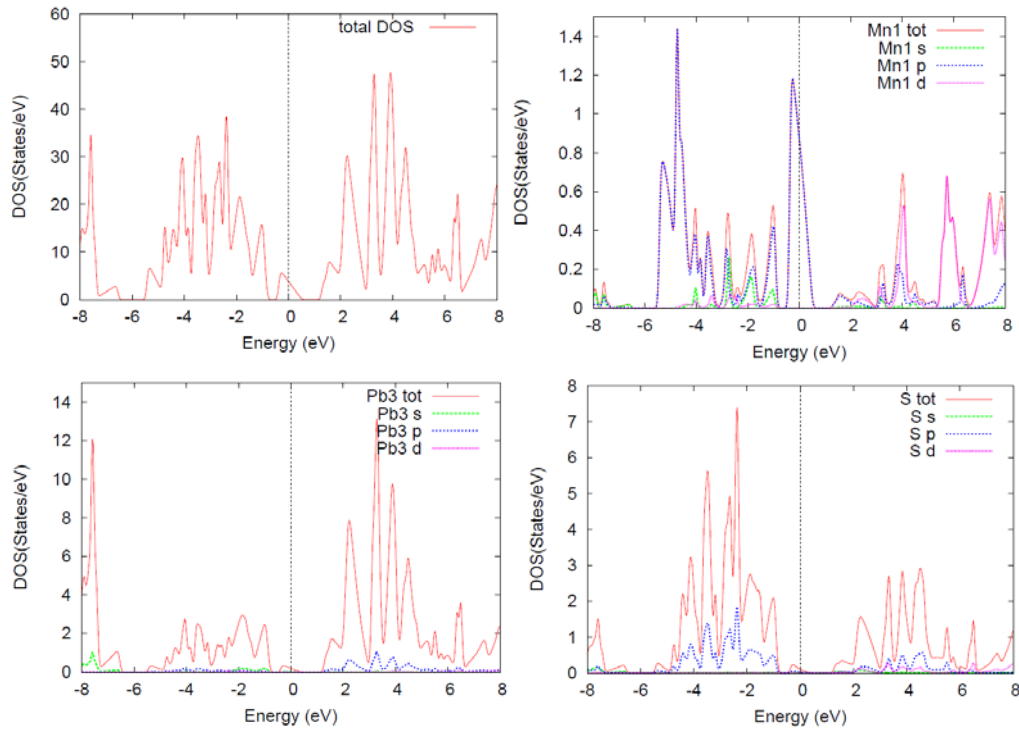


Fig. 2. Calculated total and partial density of states (DOS) for Mn doped PbS

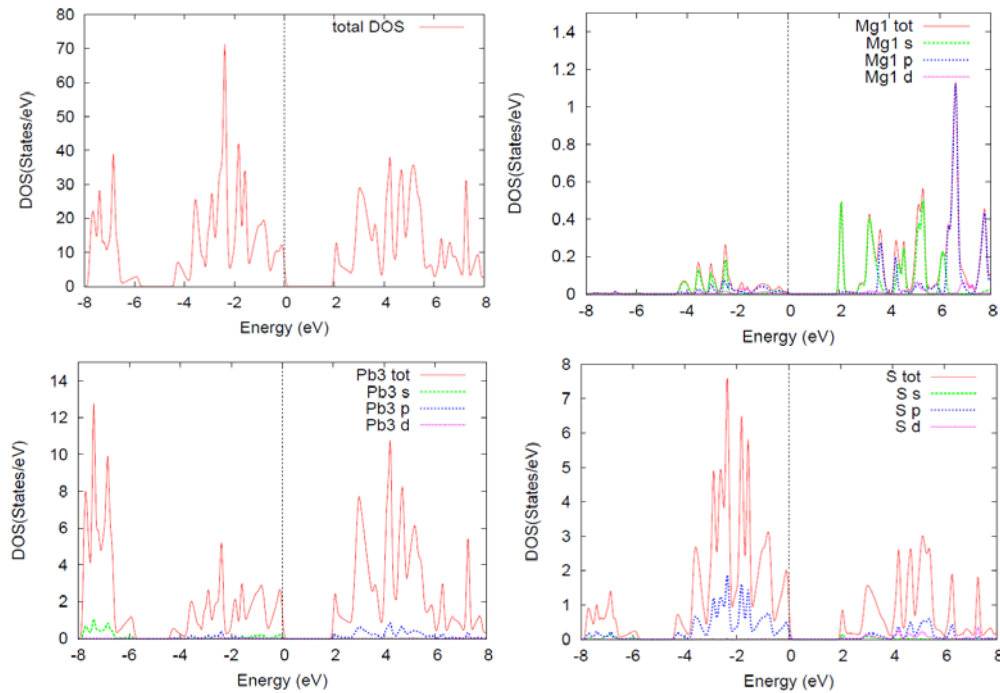


Fig. 3. Calculated total and partial density of states (DOS) for Mg doped PbS

### 3.2. Optical properties

In this section we study the optical properties of Mg doped PbS which has a semiconductor behavior. The optical properties were investigated within mBJ potential. The other optical constants, like the refractive index, the extinction coefficient and the reflectivity, are then

calculated from the dielectric function. The dielectric function  $\epsilon(\omega)$  represents the collective excitations of the Fermi Sea like the volume and surface plasmons [22]. Moreover, this function depends on the electronic structure of a material, and the determination of the behavior of the band of a solid. The dielectric function has real (dispersive) and an imaginary (absorptive) parts [23]:

$$\varepsilon(\omega) = \varepsilon_1(\omega) + i\varepsilon_2(\omega) \quad (1)$$

The imaginary part  $\varepsilon_2(\omega)$  of the dielectric function is given by [24]:

$$\varepsilon_2(\omega) = \left( \frac{4\pi^2 e^2}{m^2 \omega^2} \right) \sum_{i,j} \int |\langle i|M|j \rangle|^2 f_i(1-f_j) \delta(E_f - E_i - \eta\omega) d^3k \quad (2)$$

where  $i$  and  $j$  the initial and final states,  $M$  is the dipole matrix,  $f_i$  the Fermi distribution function for the  $i^{\text{th}}$  state and  $E_i$  the energy of the electron at the  $i^{\text{th}}$  state. The real part  $\varepsilon_1(\omega)$  is given by the Kramers–Kronig relation [25]:

$$\varepsilon_1(\omega) = 1 + \frac{2}{\pi} P \int_0^{\infty} \frac{\omega' \varepsilon_2(\omega')}{\omega'^2 - \omega^2} d\omega' \quad (3)$$

where  $P$  is the principal value of the integral.

The refractive index  $n(\omega)$  and the extinction coefficient  $k(\omega)$ , are calculated from the real and imaginary part of the dielectric function as seen in Ref. [26]:

$$n(\omega) = \left\{ \frac{\varepsilon_1(\omega)}{2} + \frac{\sqrt{\varepsilon_1^2(\omega) + \varepsilon_2^2(\omega)}}{2} \right\}^{\frac{1}{2}} \quad (4)$$

$$k(\omega) = \left\{ \frac{\sqrt{\varepsilon_1^2(\omega) + \varepsilon_2^2(\omega)} - \varepsilon_1(\omega)}{2} \right\}^{\frac{1}{2}} \quad (5)$$

Using optical constants  $n(\omega)$  and  $k(\omega)$ , the reflectivity  $R(\omega)$  was calculated by the following equation:

$$R(\omega) = \frac{(n-1)^2 + k^2}{(n+1)^2 + k^2} \quad (6)$$

Maximum value of  $\varepsilon_1(\omega)$  is 13.72 at 2.93eV for Mg doped PbS (Fig. 4). We observe a decrease of  $\varepsilon_1(\omega)$  is observed and after that it becomes negative, in this energy range, the material has metallic behavior. Refractive index  $n(\omega)$  has been calculated, which has similar profile of  $\varepsilon_1(\omega)$ . Fig. 5 shows that the Mg doped PbS have the main peak in  $\varepsilon_2$  at 3.64eV. The imaginary part  $\varepsilon_2$  was obtained from the electronic calculation. The energy loss  $L(\omega)$  is important to the description of microscopic and macroscopic properties of materials. The major peak in the

$L(\omega)$  spectrum is identified as the plasmon peak, The energy-loss function  $L(\omega)$  is given by [27]:

$$L(\omega) = \varepsilon_2(\omega) / [\varepsilon_1^2(\omega) + \varepsilon_2^2(\omega)] \quad (7)$$

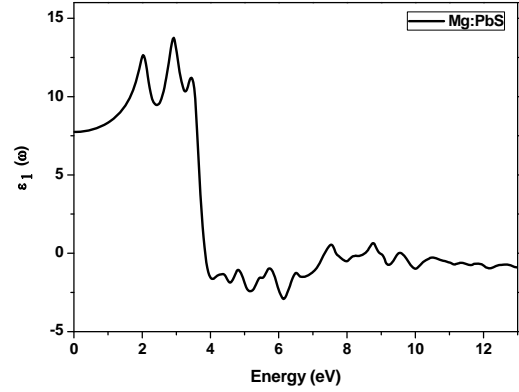


Fig. 4. Real part  $\varepsilon_1(\omega)$  of the theoretical dielectric function for Mg doped PbS

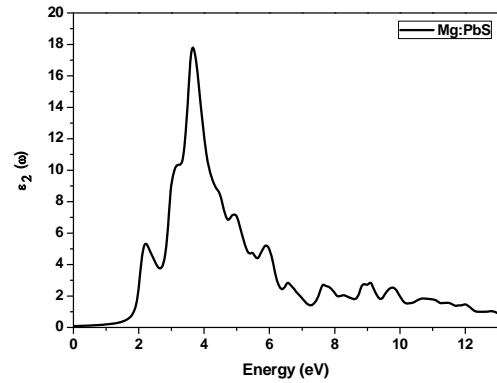


Fig. 5. Imaginary part  $\varepsilon_2(\omega)$  of the theoretical dielectric function for Mg doped PbS

In Fig. 6 the calculated energy loss  $L(\omega)$  for Mg doped PbS is presented. The major peak occurs at 7.27eV. This major peak is related to the bulk Plasmon [28]. The bulk plasmon peak as obtained from the  $L(\omega)$  spectra can be used to give information about the strain in the solid [29]. In Fig. 7, we observe an abrupt reduction is observed in the reflectivity spectra  $R(\omega)$  at  $\approx 7.44$ eV, which is due to the occurrence of a collective plasma resonance [30]. The calculated refractive index  $n(\omega)$  is shown in Fig. 8(a), from which the values of the static refractive index is obtained at  $n(0) = 2.79$ . Generally, a refractive index  $n(\omega)$  smaller than unity ( $v_g = \frac{c}{n}$ ) indicated that the group velocity of the incident radiation is higher than the speed of light [31]. The refractive index  $n(\omega)$  is related to the density and the local polarizability of this material [32]. From Fig. 8(b), we observe local maxima of the extinction

coefficient  $k(\omega)$  is for an energy of 3.81eV.

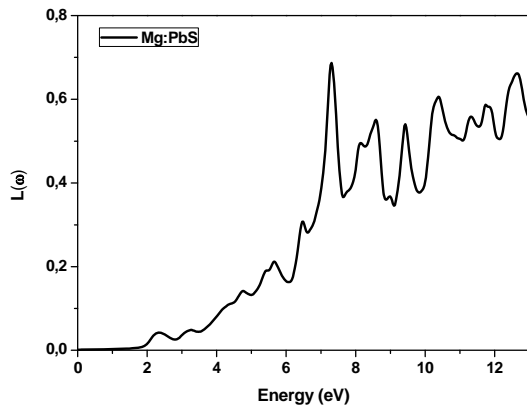


Fig. 6. Energy loss function  $L(\omega)$  of Mg doped PbS

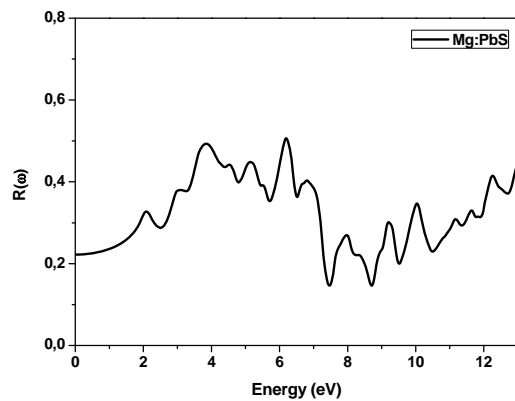


Fig. 7. Reflectivity spectra  $R(\omega)$  of Mg doped PbS

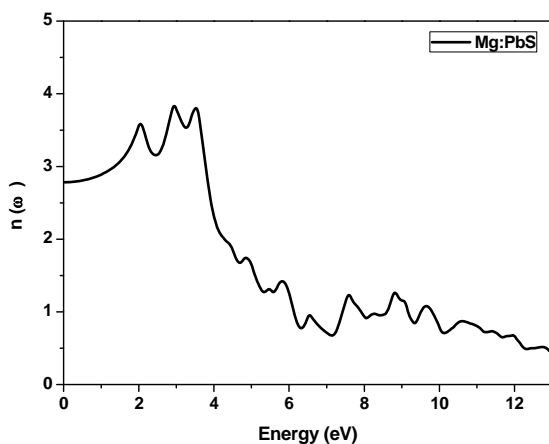


Fig. 8(a). Refractive index  $n(\omega)$  of Mg doped PbS

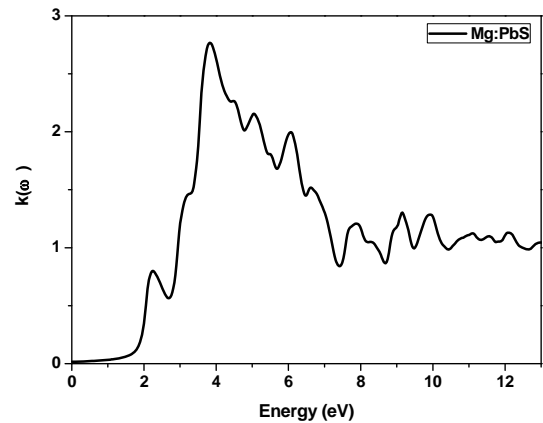


Fig. 8(b). Extinction coefficient  $k(\omega)$  of Mg doped PbS

#### 4. Conclusion

We have investigated the physical properties of Mn and Mg doped PbS. Band gap dependent optical constants like the dielectric function, the refractive and reflectivity were investigated based on the modified Becke-Johnson approach. We have found that the band gap of pure PbS is 0.9 eV, the Mn doped PbS presents a metallic behavior, and the Mg doped PbS reveals a semiconducting nature with a band gap of about 2 eV. Hence, it is found that, the calculated fundamental band gap of PbS is close to the experimental one. The maximum value of  $\epsilon_1 = 13.72$  at 2.93 eV for Mg doped PbS. We have also calculated the refractive index  $n(\omega)$ , the extinction coefficient  $k(\omega)$ , the energy-loss  $L(\omega)$  and the reflectivity  $R(\omega)$ . The value of the static refractive index is  $n(0) = 2.79$  for Mg doped PbS. The calculated electronic structure and optical properties obtained in our investigation demonstrate promising applications of Mg doped PbS for optoelectronic technologies.

#### Acknowledgements

The authors are thankful to the Deanship of Scientific Research- Research Center at King Khalid University in Saudi Arabia, for funding this research (code number: G.R.P-382-1438/2017).

#### References

- [1] E. Pentia, L. Pintilie, T. Botila, I. Pintilie, A. Chaparro, C. Maffiotte, *Thin Solid Films*. **434**, 162 (2003).
- [2] J. Seo, M. J. Cho, D. Lee, A. N. Cartwright, P. N. Prasad, *Adv. Mater.* **23**, 3984 (2011).
- [3] S. Abe, K. Masumoto, K. Suto, *Cryst. Growth* **181**, 367 (1997).

- [4] R. Joshi, H. Sehgal, *Nanotechnology* **14**, 592 (2003).
- [5] R. Silva, P. Morais, H. Sullasi, W. Ayta, F. Qu, N. Dantas, *J. Alloy. Compd.* **483**, 204 (2009).
- [6] V Krishnakumar, G. Shanmugam, R. Nagalakshmi, *J. Phys. D: Appl. Phys.* **45**, 165102 (2012).
- [7] A. Gassoumi, S. Alleg, N. Kamoun-Turki, *J. Mol. Struct.* **1116**, 67 (2016).
- [8] B. Touati, A. Gassoumi, S. Alfaify, N. Kamoun-Turki, *Mat. Sci. Semicon. Proc.* **34**, 82 (2015).
- [9] B. Touati, A. Gassoumi, I. Dobryden, M. M. Natile, A. Vomiero, N. Kamoun-Turki, *Superlattice Microst.* **97**, 519 (2016).
- [10] G. Dong, M. Zhang, W. Lan, P. Dong, H. Yan, *Vacuum* **82**, 1321 (2008).
- [11] J. Bang, H. Yang, P. Holloway, *Nanotechnology* **17**, 973 (2006).
- [12] G. Long, B. Barman, S. Delikanli, Y. Tsai, P. Zhang, A. Petrou, H. Zeng, *Appl. Phys. Lett.* **101**, 062410 (2012).
- [13] D. Koller, F. Tran, P. Blaha, *Phys. Rev. B* **83**, 195134 (2011).
- [14] W. Khan, A. H. Reshak, *J. Mater. Sci.* **49**, 1179 (2014).
- [15] F. Tran, P. Blaha, *Phys. Rev. Lett.* **102**, 226401 (2009).
- [16] Y. Noda, K. Masumoto, S. Ohba, Y. Saito, K. Toriumi, Y. Iwata, I. Shibuya, *Acta Cryst. C* **43**, 1443 (1987).
- [17] W. Kohn, L. J. Sham, *Phys. Rev.* **140**, A1133 (1965).
- [18] D. Koelling, B. Harmon, *J. Phys. C: Sol. Stat. Phys.* **10**, 3107 (1977).
- [19] P. Blaha, K. Schwarz, G. K. H. Medsen, D. Kvasnicka, J. Luitz, Karlheinz Schwartz, *Techn. Universitat, Wien, Austria* (2001).
- [20] X. Tan, H. Shao, T. Hu, G. Liu, S. Ren, *J. Phys.: Condens. Matter.* **27**, 095501 (2015).
- [21] C. Rajashree, A. R. Balu, V. S. Nagarethinam, *J Mater Sci: Mater Electron.* **27**, 5070 (2016).
- [22] B. Amin, R. Khenata, A. Bouhemadou, I. Ahmad, M. Maqbool, *Physica B* **407**(13), 2588 (2012).
- [23] J. S. Tell, *Phys. Rev.* **104**, 1760 (1956).
- [24] P. Puschnig, C. Ambrosch-Draxl, *Phys. Rev. B* **66**, 165105 (2002).
- [25] Y. P. Yu, M. Cardona, *Fundamentals of semiconductors: physics and materials properties*, 2nd edn. springer-verlag, Berlin (1999), pp 233.
- [26] M. Dressel, G. Gruner, *Electrodynamics of solids: optical properties of electrons in matter*, Cambridge University Press, UK (2002).
- [27] A. H. Reshak, S. A. Khan, Z. A. Alahmed, *Optical Materials* **37**, 322 (2014).
- [28] A. H. Reshak, M. Shalaginov, Y. Saeed, I. V. Kityk, S. Auluck, *J. Phys. Chem. B* **115**, 2836 (2011).
- [29] J. Palisaitis, C.L. Hsiao, M. Junaid, J. Birch, L. Hultman, P. O. Å. Persson, *Phys. Rev. B* **84**, 245301 (2011).
- [30] G. Murtaza, S. K. Gupta, T. Seddik, R. Khenata, Z. A. Alahmed, R. Ahmed, H. Khachai, P. K. Jha, S. Bin Omran, *J. Alloy. Compd.* **597**, 36 (2014).
- [31] G. Murtaza, G. Sadique, H. A. Rahnamaye, A. Abad, M. N. Khalid, S. Naeem, A. Afaq, B. Amin, I. Ahmad, *Physica B* **406**, 4584 (2011).
- [32] N. M. Balzaretti, J. A. Jornada, *Solid State Commun.* **99**, 943 (1996).

---

\*Corresponding author: abdelaziz.gassoumi@gmail.com